41st Annual Frequency Control Symposium - 1987

ESTIMATING COMBINED ERRORS DUE TO PROPAGATION AND EPHEMERIS AND THEIR EFFECT ON TIME AND FREQUENCY TRANSFER

by

David W. Allan* and Lin Ping-ping†

*National Bureau of Standards
Boulder, Colorado 80303

and

†Beijing Institute of Radio Measurement
Beijing, China

ABSTRACT

We now have a global network of timing centers with frequency standards having stabilities of a few parts in 10^{14} which are monitoring the GPS. It has been shown that by taking differences of the common-view time differences between two timing centers and between pairs of satellites, one can arrive at a statistically optimum estimate for a weighting factor for each common-view path. With this approach, GPS common-view measurement noise of a few parts in 10^{14} is achievable for an integration time of 1 day.

Using the above weighting factors, this paper developes an algorithm for estimating a weighted linear error of the differential ephemeris plus propagation errors for each satellite. This can be done between any pair of timing centers which have receivers and clocks with adequate stability. Since most of the time transfer receivers operate at the L1 frequency (1.575 GHz), this technique reveals information regarding the accuracy of the ionospheric models broadcast at this frequency as part of the GPS data word.

Once the individual satellite's differential propagation and ephemeris errors are estimated, the statistical properties of each can be combined to obtain a statistically weighted estimate of the common-view measurement variations limiting the comparison of the clocks between the two remote sites. Optimum statistical weighting yields a significantly better measurement noise than can be obtained from a simple average. For example, between NRC in Ottawa, Canada and NBS in Boulder, Colorado demonstrated stabilities of $\bar{\sigma}_y(\tau) = 1 \times 10^{-14}\ \tau^{-3/2}$, where τ is in day's, have been achieved. This is equivalent to a white time modulation noise of less than 1 ns sampled once per day. On the other hand, without proper care in the data processing errors can accumulate to several tens of nanoseconds in common-view time comparisons.

INTRODUCTION

The goal of this paper is to investigate the limitations caused by the propagation and ephemeris errors associated with time and frequency comparisons between remote clocks via GPS satellites in common view. The common-view technique capitalizes on cancellation of some errors as a given satellite is viewed at the highest angle -- limited by other scheduling constraints -- between the two remote locations.[1,2] Typically L1 (1.575 GHz) frequency receivers are employed. If the tracking schedules for comparing the clocks at the remote sites are identical, then the GPS clock error cancels perfectly. Because the vectors are not far from parallel, a significant amount of the ephemeris error is cancelled. The correlation distances for the ionosphere extend only to about 1000 kilometers[3]; hence, for global time comparisons, cancellation of ionospheric errors seems not to be significant except as they occur through the modeling. The broadcast model for the ionospheric delay is used in the common-view calculations, and it appears that these modeling errors are the largest contributors to the inaccuracy of time and frequency transfer via this technique.

In the context of this paper there are four concepts that need to be defined: time stability, time accuracy, frequency stability, and frequency accuracy. Specifically, in this paper we address only stability and accuracy of the GPS common-view measurement technique and not that of the remote clocks. Our goal again is to see how well we can compare the time and frequency of the remote clocks using this technique as limited by the propagation and ephemeris errors. Time stability is a measure of the change in the measurement system time delay from one time to a time τ later. Time accuracy can be conceptualized in terms of a perfect portable clock which is used to measure the absolute time difference between the two remote clocks. Frequency stability is usually specified in terms of $\sigma_y(\tau)$ and/or modified $\sigma_y(\tau)$, (denoted $\bar{\sigma}_y(\tau)$).[4-6] Frequency accuracy of the measurement system is a measure of how well one can determine the absolute frequency difference between the two remote standards.

METHOD OF ANALYSIS

References [2&7] showed that over a given day's tracking schedule of GPS satellites, two remote clocks having a set of common-view values can be compared with a day-to-day time stability of a few nanoseconds. On a given day if the difference of the time difference between these two remote clocks is calculated from data obtained through two different GPS satellite vehicles (SV), then the times of these remote clocks drop out of the equations and we are left only with the difference in the common-view propagation and ephemeris errors between these two

tracks. For most of the international timing centers the effect of the remote clocks on this assumption amounts to only a few nanoseconds.

We will denote the two remote clock sites as A and B. At sites A and B we measure, respectively, time differences at a time t_i of clock A and B minus GPS:

$$x_{AG}(t_i) = x_A(t_i) - x_G(t_i) - x_D(t_i) \qquad (1)$$

and

$$x_{BG}(t_i) = x_B(t_i) - x_G(t_i) - x_D(t_i), \qquad (2)$$

where x_A, x_B, and x_G are the true time deviations for clocks A, B, and GPS via the i^{th} SV respectively, and the x_Ds are the errors at A and B between these measures and the truth. Subtracting (2) from (1) gives us the common-view estimate equation for the time difference between clocks A and B:

$$x_{AB}(t_i) = x_A(t_i) - x_B(t_i) - x_{D_{AB_i}}(t_i), \qquad (3)$$

where $x_{D_{AB_i}}(t)$ is now the differential delay error via SV_i. It has been shown that the differential delay errors are significantly smaller than either of the error terms in equations (1) and (2), hence, the value of common view for time and frequency comparisons between remote clocks [2].

We have a similar measurement at a time t_j of the common-view estimate of the time difference $x_{AB}(t_j)$ via SV_j:

$$x_{AB}(t_j) = x_A(t_j) - x_B(t_j) - x_{D_{AB_j}}(t_j). \qquad (4)$$

Subtracting (4) from (3) we obtain

$$x_{AB}(t_{ij}) = x_A(t_i) - x_A(t_j) + x_B(t_i) - x_B(t_j) - x_{D_{AB_{ij}}}(t_{ij}). \qquad (5)$$

If $t_i = t_j$ then, of course, the first four terms on the right of (5) cancel in pairs. In a typical pass of the GPS constellation the maximum value for $| t_i - t_j |$ is about 6 hours or less. For typical high-performance cesium-beam frequency standards employed at international timing centers the rms contribution of the first four terms is about 2 ns or less for a set of such passes taken as a time series.

If clocks A and B have a frequency difference, this will cause a bias in the value given by (5), which will have no effect on the statistical analysis to follow, but can have an effect on the linear estimate. If the frequency difference changes outside of the normal noise of the clocks, then that change will have an effect on the statistics.

Given that each path i and j is nominally independent of the others, and given the above conditions, let us simplify (5) to

$$x_{AB}(t_{ij}) \approx x_{ji}(\bar{t}_{ij}), \qquad (6)$$

where $\bar{t}_{ij}$ is the average of the track times t_i and t_j. As shown in reference [4] we can do N-corner statistics on (6) to determine the optimum weight, w_i, for each common-view track.

Let us next assume that the variance of the deviations of $x_{D_{AB_i}}(t)$ is proportional to the linear deviation. If this is true then we can write as an estimate of the jth linear deviation,

$$\hat{x}_{jo} = \sum_{i=1}^{n} w_i (x_{ji} - x_{io}), \qquad (7)$$

where there are n values from the SVs on a given day and x_{io} is the true deviation of the differential-delay common-view error. The above assumption yields

$$\sum_{i=1}^{n} w_i \, x_{io} = 0 ; \qquad (8)$$

hence, even though x_{io} is not known, if our assumptions are valid, we can estimate the linear deviation as in (7).

Multipath and coordinate errors in the GPS receivers at A and B can also bias the value calculated in (5). Since these are nominally constant they will not affect the variances--only the linear estimates.

Since the largest error in the linear deviation for common-view time and frequency transfer is believed to be in the ionospheric modelling on the GPS L1 frequency, we have performed a global analysis of the estimate given by equation (7). The stations used in the analysis were picked from around the world. These stations include the following:

TABLE I

	TIME CENTER	WEST LONGITUD.	LATITUDE
CSIRO	Commonwealth Scientific and Industrail Research Organization Australia	208°.8	33°.8S
NBS	National Bureau of Standards Boulder, Colorado	105°.3	40°.0N
NRC	National Research Council Ottawa, Canada	75°.9	45°.4N
PTB	Physikalisch-Technische Bundesanstalt Braunschweig, West Germany	307°.7	52°.3N
RRL	Radio Research Laboratory Tokyo, Japa	220°.5	35°.7N
USNO	US Naval Observatory Washington, D.C.	77°.1	38°.9N

Figure 1 is a plot of the day-by-day estimate of the combined propagation and ephemeris common-view errors between USNO and NBS via SV 12 (NAVSTAR 10) given by equation (7). The Fourier frequency spectrum is characterized by white-noise phase modulation (PM); hence, filtering is appropriate in order to see the low-frequency characteristics of the data. A 30-day exponential filter was chosen through which to plot the day-by-day estimates given by equation 7. Figure 2 shows a plot of data obtained through both NAVSTAR 10 and the other vehicles available between Washington, D.C. and Boulder, Colorado using the USNO

and NBS L1 receivers. If the residuals are white noise PM, the measurement noise is given by [6]

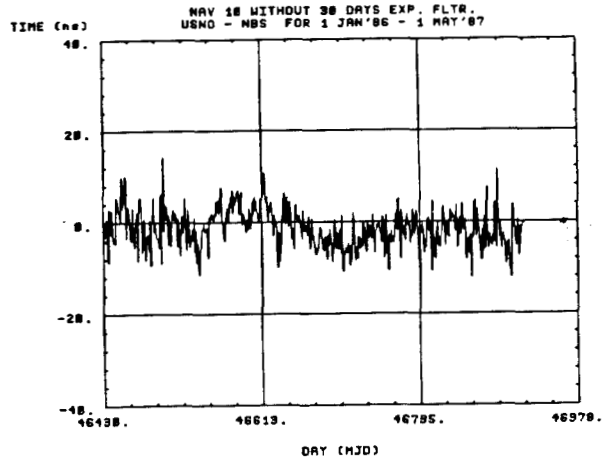

FIGURE 1 A plot of the daily estimate via equation 7 of the differential ephemeris plus propagation errors for GPS common-view measurements between Boulder, Colorado and Washington D.C. via NAVSTAR 10.

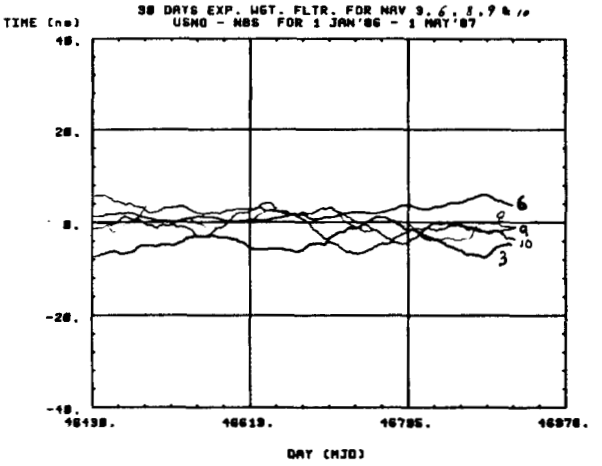

FIGURE 2 A plot of a filtered estimate via equation 7 of the differential ephemeris plus propagation errors for GPS common-view measurements between Boulder, Colorado and Washington D.C. via the different NAVSTAR satellites indicated.

$$x_{rms}(\tau_o) = \frac{1}{\sqrt{3}}\ \tau\ \sigma_y(\tau) = \frac{\tau^{3/2}}{(3\ \tau_o)^{1/2}}\ \bar{\sigma}_y\ (\tau)\ , \qquad (9)$$

where τ_o is the data spacing i.e., 1 sidereal day. The composite measurement noise is given by

$$x_{rms}\ (\tau_o) = [\sum_{i=1}^{n} \frac{1}{\sigma^2_i}]^{-1/2}\ , \qquad (10)$$

where the σ_i^2 come from the N-cornered-hat statistical analysis using (6). The average standard deviation of the residuals across the different SVs is listed in Table 2. Comparing it to the composite measurement noise, which is also listed, one obtains a feel for the benefit of performing a combined optimal weighted estimate to obtain improved time stability. This factor ranges between 3 and 14 for the data in this paper. Equation (9) gives the relationship between the time stability and the frequency stability. The time accuracy is probably more closely related to the standard deviation of the residuals as listed in Table 2. The frequency accuracy of the measurement, on the other hand, will be given by the magnitude of the integration time chosen in measuring the frequency difference between clocks A and B. The value of $\bar{\sigma}_y(\tau)$, once a weighted set of the common-view tracks is taken, will be an estimate of that accuracy. This measurement accuracy has been demonstrated to be significantly better than the accuracy of the best primary frequency standards in the world.

Figure 3 shows the smoothed deviations of the residuals for the path from Australia to Tokyo. We

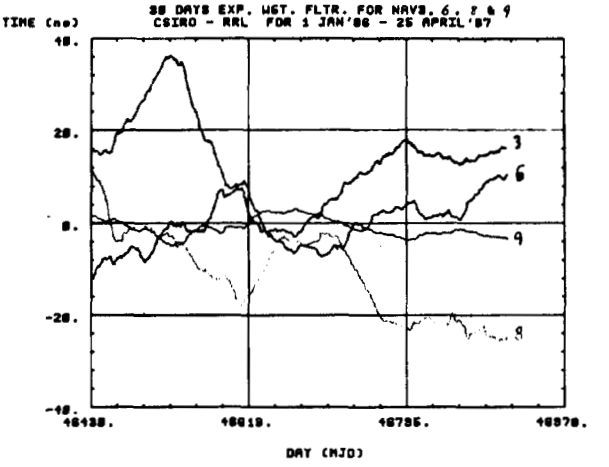

FIGURE 3 A plot of a filtered estimate via equation 7 of the differential ephemeris plus propagation errors for GPS common-view measurements between Australia and Japan via the different NAVSTAR satellites indicated.

see a lot more low-frequency variations and some evidence for systematic errors in these data. The next common-view path shown in Figure 4 is from Tokyo to Boulder, Colorado between RRL and NBS. Notice an apparent annual term for the residuals with NAVSTAR 10, as well as with NAVSTAR 6. Figure 5 shows data for the common-view path across Asia from RRL to PTB. Figure 6 shows comparisons between PTB and NBS on a

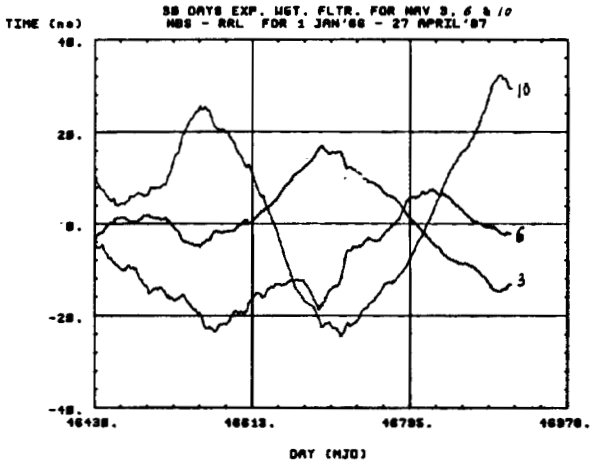

FIGURE 4 A plot of a filtered estimate via equation 7 of the differential ephemeris plus propagation errors for GPS common-view measurements between Colorado and Japan via the different NAVSTAR satellites indicated.

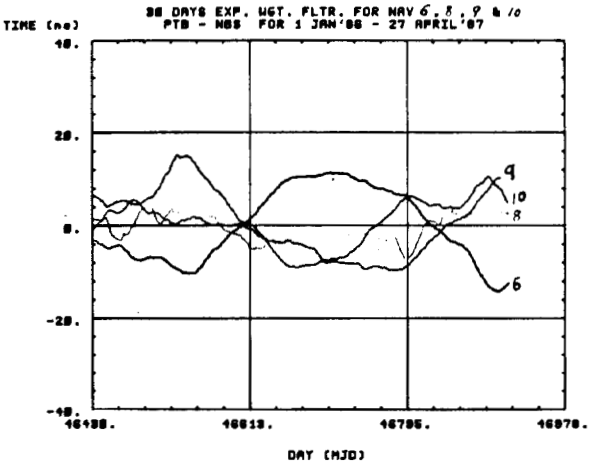

FIGURE 6 A plot of a filtered estimate via equation 7 of the differential ephemeris plus propagation errors for GPS common-view measurements between West Germany and Colorado via the different NAVSTAR satellites indicated.

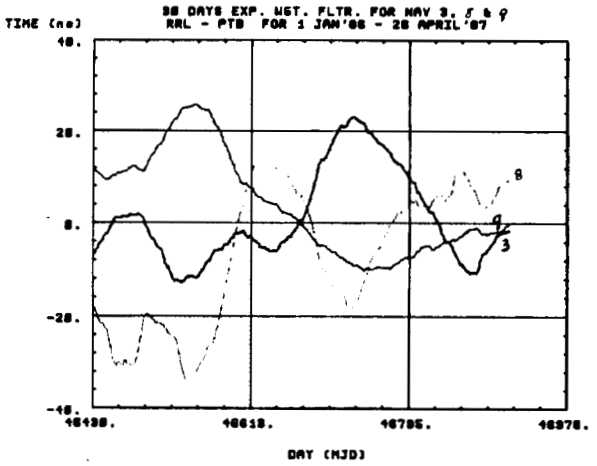

FIGURE 5 A plot of a filtered estimate via equation 7 of the differential ephemeris plus propagation errors for GPS common-view measurements between West Germany and Japan via the different NAVSTAR satellites indicated.

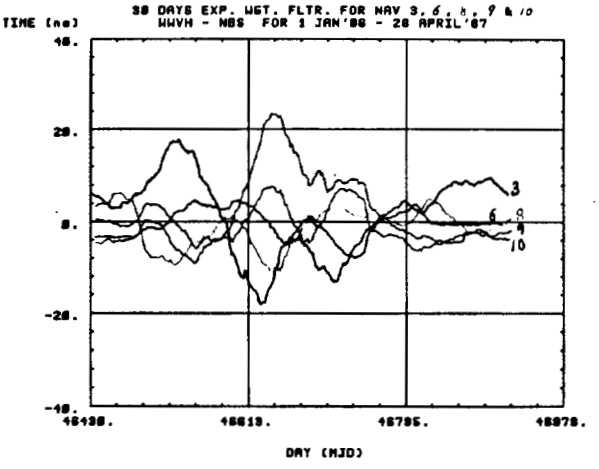

FIGURE 7 A plot of a filtered estimate via equation 7 of the differential ephemeris plus propagation errors for GPS common-view measurements between Hawaii and Colorado via the different NAVSTAR satellites indicated.

path across the Atlantic plus the continental US. These data also show an apparent annual variation with NAVSTAR 6 and 10 of about 20 ns.

The path between Hawaii and Boulder was chosen because of the proximity of the clock at WWVH to the equator -- placing greater demands on the ionospheric modeling. The peak-to-peak scatter shown in Figure 7 seems to be a bit larger and the variability seems to be higher. No annual term is evident. In contrast the comparison across the continental US between Ottawa, Canada and Boulder, Colorado involves a very high-latitude station. These data, shown in Figure 8, are quite different and show very small variability and an indication of significant biases which could be due to multipath or coordinate problems at one or both of the sites.

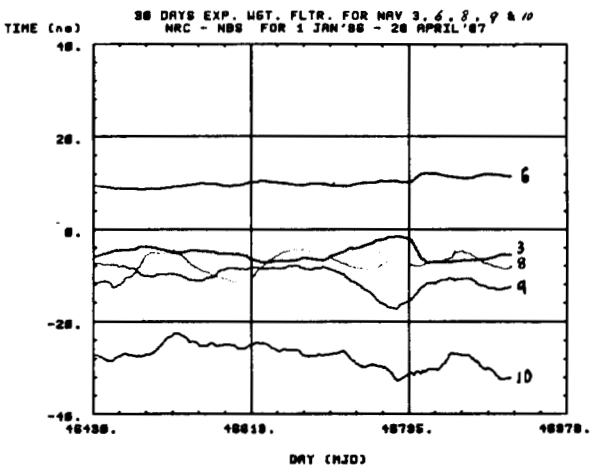

FIGURE 8 A plot of a filtered estimate via equation 7 of the differential ephemeris plus propagation errors for GPS common-view measurements between Ottawa, Canada and Boulder, Colorado via the different NAVSTAR satellites indicated.

Conclusion

Table 2 lists the paths i.e., the end locations of clocks A and B, the standard deviation of the filtered data over the last 100 days and the weighted measurement noise for each of the common-view paths studied. Global time comparison accuracies of about 20 nanoseconds or less are available from a weighted set of GPS satellites used in common view. Time stabilities are typically only a few nanoseconds for global time comparisons. Frequency stabilities may be characterized by the square root of the modified Allan variance, $\sigma_y(\tau)$, equal to a few parts in 10^{14} times $\tau^{-3/2}$ (τ in days) for integration times from one day to a couple of weeks. The full accuracy of state-of-the-art primary frequency standards is available at a remote site through a weighted average of the GPS satellites used in common view i.e., values less than 1 part in 10^{14} are achievable for integration times of a few days.

TABLE 2

PATH	AVERAGE STANDARD DEVIATION (ns)	DAY-TO-DAY MEASUREMENT NOISE (ns)
USNO - NBS	4.2	1.4
CSIRO - RRL	18.6	3.4
NBS - RRL	20.5	5.2
RRL - PTB	12.1	4.8
PTB - NBS	8.5	2.0
WWVH - NBS	5.9	2.3
NRC - NBS	19.0	1.4

REFERENCES

1. Allan, D.W., Weiss, M.A., "Accurate Time and Frequency Transfer During Common-View of a GPS Satellite", Proc. 34th Ann. Freq. Control Symp., USAERADCOM, Ft. Monmouth, N.J. 07703, May 1980.

2. D.W. Allan, D.D. Davis, M.A. Weiss, A. Clements, Bernard Guinot, Michel Granveaud, K. Dorenwendt, B. Fischer, P. Hetzel, Shinko Aoki, Masa-Katsu Fujimoto, L. Charron, and N. Ashby, "Accuracy of International Time and Frequency Comparisons Via Global Positioning System Satellites in Common-View", IEEE Transactions on Instrumentation and Measurement, Vol. IM-34, No. 2, June 1985.

3. Klobuchar, J.A. (1978), "Ionospheric Effects on Satellite Navigation and Air Traffic Control Systems," NATO AGARD proceedings, Lecture Series No. 93, Recent Advances in Radio and Optical Propagation for Modem Communication, Navigation, and Detection Systems.

4. Barnes, J.A., Chi, A.R., Cutler, L.S., Healey, D.J., Lesson B., McGunigal, T.E., Mullen, Jr., J.A., Smith, W.L., Sydnor L., Vessot, R.F.C., Winkler, G.M., "Characterization of Frequency Stability," Proc. IEEE Tran. on Instrumentation and Measurement", Vol. IM-20, 105, NBS Technical Note 394, 1971.

5. Lesage, P., Ayi, T., "Characterization of Frequency Stability: Analysis of the Modified Allan Variance and Properties of Its Estimate," IEEE Transactions on Instrumentation and Measurement", Vol. IM-33, No. 4, December 1984, pp. 332-336.

6. Allan, D.W., "Time and Frequency Characterization, Estimation Prediction of Precision Clocks and Oscillators," IEEE, Ultrasonics Ferroelectrics and Frequency Control, Special Issue on Frequency Control, Nov. 1987.

7. Weiss, M.A., and Allan, D.W., "An NBS Calibration Procedure for Providing Time and Frequency at a Remote Site by Weighting and Smoothing of GPS Common View Data," Proceedings of the CPEM Conference, Gaithersburg, MD, June 1986.